MOLECULAR AND CELLULAR BIOLOGY, Apr. 1983, p. 712–719
0270-7306/83/040712-08$02.00/0

Vol. 3, No. 4

Fate of Microfilaments in Vero Cells Infected with Measles Virus and Herpes Simplex Virus Type 1

ELLIOTT BEDOWS,[1]* K. M. K. RAO,[2]† AND MICHAEL J. WELSH[3]

Department of Epidemiology, School of Public Health,[1] and Departments of Anesthesiology,[1] Pathology,[2] and Anatomy and Cell Biology,[3] School of Medicine, University of Michigan, Ann Arbor, Michigan 48109

Received 16 July 1982/Accepted 6 December 1982

In herpes simplex virus type 1-infected Vero cells, reorganization of microfilaments was observed approximately 4 h postinfection. Conversion of F (filamentous) actin to G (globular) actin, as assessed by a DNase I inhibition assay, was continuous over the next 12 to 16 h, at which time a level of G actin of about twice that observed in uninfected cells was measured. Fluorescent localization of F actin, using 7-nitrobenz-2-oxa-1,3-diazole (NBD)-phallacidin, demonstrated that microfilament fibers began to diminish at about 16 to 18 h postinfection, roughly corresponding to the time that G actin levels peaked and virus-induced cytopathology was first observable. In measles virus-infected cells, no such disassembly of microfilaments occurred. Rather, there was a modest decrease in G actin levels. Fluorescent localization of F actin showed that measles virus-infected Vero cells maintained a complex microfilament network characterized by fibers which spanned the entire length of the newly formed giant cells. Disruption of microfilaments with cytochalasin B, which inhibits measles virus-specific cytopathology, was not inhibitory to measles virus production at high multiplicities of infection (MOI) but was progressively inhibitory as the MOI was lowered. The carbobenzoxy tripeptide SV-4814, which inhibits the ability of Vero cells to fuse after measles virus infection, like cytochalasin B, inhibited measles virus production at low MOI but not at high MOI. Thus, it appears that agents which affect the ability of Vero cells to fuse after measles virus infection may be inhibitory to virus production and that the actin network is essential to this process.

Cellular morphology is generally altered after acute virus infection. This cytopathic effect (CPE) is most often expressed as cellular rounding and a more vacuolized and granular appearance of the cell cytoplasm, as seen with phase-contrast optics. However, paramyxoviruses usually demonstrate giant cell or syncytia formation as a consequence of their cytopathology. Morphological changes in the cell are coincident with cytoskeletal alteration (4, 26). It is not clear whether changes in the cytoskeletal structure observed after virus infection are a passive result of virus-induced changes in cell metabolism or whether viruses actively change these cellular structures to facilitate their own replication. Some investigators have observed that virus replication in culture proceeds almost normally in cells which have been treated with microfilament-disrupting agents, such as cytochalasin B (CB) (9, 12), once the virus has entered the cell (5). Similarly, others (17) have demonstrated that mutants of Newcastle disease virus which are deficient in their ability to produce cytopathology still retain infectivity. These results suggest that the role of microfilaments during virus infection may be passive. However, other workers have shown that actin filaments function in the control of movement of measles virus envelope proteins on the surface of infected cells (6). Furthermore, Tyrrell and Ehrnst (27), using monospecific antisera to the N and M proteins of measles virus, showed that the normally observed cocapping of these proteins with the capping of surface virus glycoproteins was inhibited by CB in chronically infected human cells. In the present communication, we describe changes in the microfilament network of Vero cells infected with either of two human pathogens, measles virus or herpes simplex virus type 1 (HSV), and demonstrate that microfilaments may play either an active or passive role in viral etiology depending upon the type and multiplicity of infection (MOI) of virus used in the experiment.

† Present address: Clinical Chemistry Laboratory, Department of Pathology, University of Pittsburgh, Pittsburgh, PA 15261.

MATERIALS AND METHODS

Cells. Vero cells (2) were grown in Eagle minimal essential medium containing 10% fetal calf serum and

100 μg of penicillin per ml and 100 μg of streptomycin per ml. Cells were passaged with 1:8 dilutions weekly.

Virus. Measles virus was prepared as previously described (2). The KOS strain of HSV, obtained from M. Levine, University of Michigan, was also prepared in Vero cells by the same procedure.

Plaque assay. Vero cells were grown in 25-cm^2 flasks (Corning Glass Works, Corning, N.Y.). When the cells were approaching confluency, they were inoculated with 0.2 ml of the virus suspension to be tested. After virus adsorption for 1 h at 37°C, the virus inoculum was removed, and the monolayers were washed once with calcium-free diluent and overlaid with minimal essential medium containing 2% fetal bovine serum, 2% Bacto-agar (Difco Laboratories, Detroit, Mich.), and antibiotics. After incubation at 37°C for either 4 days for HSV or 6 days for measles virus, 3 ml of a 0.02% neutral red solution was added to the agar overlay. Cultures were incubated at room temperature for 6 h, at which time the number of plaques was determined. Each assay was performed in duplicate.

Affinity-fluorescence localization of F actin in altered cells. Localization of filamentous (F) actin in cultured cells was accomplished by using 7-nitrobenz-2-oxa-1,3-diazole (NBD)-phallacidin (Molecular Probes, Inc., Plano, Tex.) as a fluorescent affinity-probe as described by Barak et al. (1). For localization of actin, cells were cultured on glass cover slips (11 by 22 mm). Photographs of epi-illumination fluorescence or phase-contrast images of cultured cells were taken with a Vario-Orthomat camera on a Orthoplan microscope (Leitz/Opto-Metric Div. of E. Leitz Inc., Rockleigh, N.J.). Kodak high speed recording film was rated at an ASA of 1,000 and developed in Ethol 90.

Measurement of G actin and total actin. The quantity of globular (G) and total actin in the cells was determined by a DNase I inhibition assay as previously described (3). G actin was determined by lysing the cells in Tris-saline buffer (2.5×10^{-3} M; pH 7.4) containing 2% Triton X-100 and assaying for DNase I-inhibiting activity immediately after lysis. Total actin was determined by lysing the cells in an actin-dissociating buffer consisting of 1.5 M guanidine hydrochloride (GuHCl), 1 M sodium acetate, 1 mM ATP, and 1 mM calcium chloride in Tris buffer (2.5×10^{-3} M; pH 8.0) containing 2% Triton X-100. After lysis, the mixture was incubated for 5 min at 4°C. The measurement of DNase I activity was carried out as described by Laub et al. (14). It is based on the decrease in fluorescence intensity (excitation at 520 nm, emission at 602 nm) of an ethidium bromide-DNA complex, occurring as a result of DNA digestion produced by the DNase I. The assay mixture consisted of 60 μg of DNA per ml, 1.5×10^{-6} M ethidium bromide, 10^{-4} M $CaCl_2$, and 10^{-3} M $MgCl_2$ in Tris-buffer (2.5×10^{-3} M; pH 8.0). The optimal amount of DNase I was found to be 2 μg per assay. Forty micrograms of DNase I per milliliter was made up in Tris-saline buffer containing 2% Triton X-100 (enzyme buffer). One hundred microliters of the cell extract was mixed with 100 μl of the enzyme buffer, and the mixture was vortexed for 10 s. At 1 min, 100 μl of this mixture was added to 3 ml of the assay mixture and placed in a cuvette in a spectrofluorometer (SF 330; Varian Instrument Group, Palo Alto, Calif.), and the change in fluorescence (Δ fluorescence) was recorded. The end point was taken at 3 min. With each experiment, an actin standard curve was obtained, using rabbit skeletal muscle actin. The standard curve was obtained in the presence of actin-dissociating buffer (GuHCl). The linear standard was obtained in the range of 2 to 5 μg of actin. Total actin values of the cell extracts were read directly from the standard curve. The amount of actin is reported as micrograms of actin per milligram of total protein. Total proteins were determined by the method of Lowry et al. (15).

GuHCl alone significantly reduced DNase activity. Failure to recognize this effect might have been responsible for the lack of success of some workers in obtaining the total actin levels using GuHCl (18), although others have not encountered this difficulty (3, 25). In any event, under our assay conditions GuHCl did exert measurable inhibitory effects on DNase activity. Therefore, to obtain G actin values for cell lysates from the standard curve, a correction factor was applied. This was done by subtracting the difference in fluorescence between the enzyme alone and the enzyme plus dissociating buffer (i.e., [Δ fluorescence enzyme] − [Δ fluorescence enzyme + GuHCl]) from the fluorescence values obtained with the cell lysates.

Although F actin does not inactivate DNase I, it has been suggested that DNase I depolymerizes F actin upon prolonged incubation (3, 14). In fact, Laub et al. (14) have determined total cellular actin after incubation with DNase I alone for 3 h. On the other hand, Fox et al. (8) suggested that the presence of ATP is mainly responsible for the slow dissociation of F filaments and that omission of ATP in the lysing buffer prevents this depolymerizing effect. In our studies, we did not have ATP in the lysing buffer. Furthermore, the total time from the lysis of the cells to the end point of the assay was only 4 min. No dissociation of F actin was observed in this short period. In fact, we were unable to notice a significant change even after an incubation of 3 h.

Measurement of total cellular actin by PAGE. To determine whether total cell actin levels changed as a result of virus infection, the relative levels of actin in cells were measured in quadruplicate cultures. Infected or uninfected cell cultures prepared as described above were harvested by scraping. Equal amounts of cell protein were resolved by sodium dodecyl sulfate slab polyacrylamide gel electrophoresis (PAGE) by the method of Laemmli (13). Proteins were stained with Coomassie blue, and the gel lanes were scanned with an Ortec 4310 densitometer. Cellular actin levels were assessed by measuring peak heights.

Special chemicals. Carbobenzoxy tripeptide SV-4814 was a kind gift from Parke, Davis & Co., Ann Arbor, Mich., and was prepared as previously described (21). Cytochalasin B and actinomycin D were purchased from the Sigma Chemical Co., St. Louis, Mo.

RESULTS

Cellular morphology. Normal Vero cells exhibit a stellate morphology (Fig. 1A). After infection with measles virus, cell fusion occurred, leading to syncytia formation. At an MOI of 0.1, Vero cell syncytia began to form 20 to 24 h postinfection (p.i.), and all cells were fused into multinucleated giant cells within 36 h

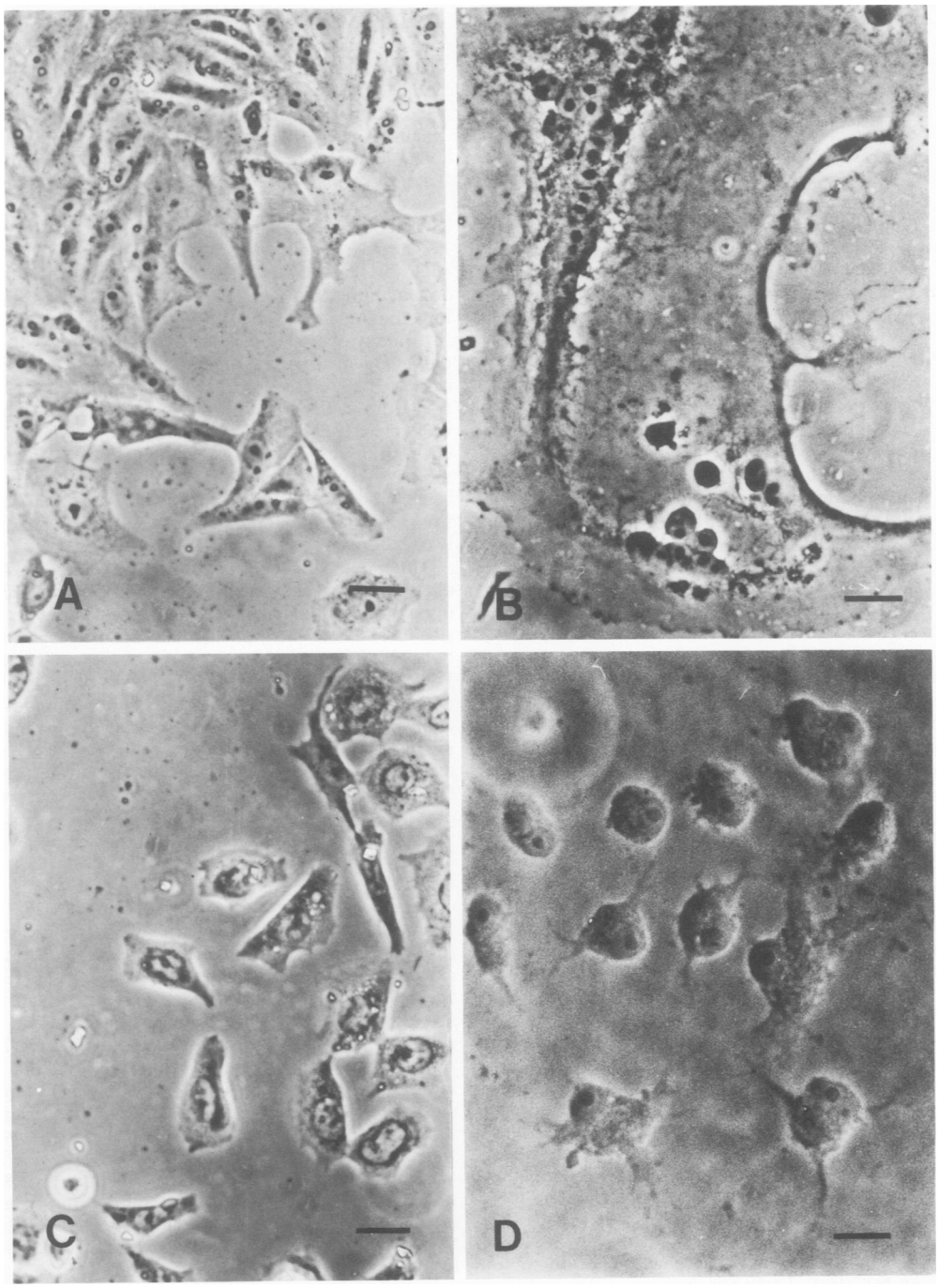

FIG. 1. Phase-contrast photography of Vero cells. (A) Untreated; (B) 22 h after infection with measles virus; (C) 16 h after infection with HSV; (D) 12 h after treatment with CB. Bar, 20 μM.

(Fig. 1B). After infection with HSV, Vero cells underwent rounding (Fig. 1C). At an MOI of 5, the first signs of HSV-specific rounding occurred 18 to 20 h p.i. with 100% CPE (total rounding with cells beginning to slough) occurring 24 to 30 h p.i. Molecular events surrounding these morphological changes are described below.

Fate of actin and microfilaments after virus infection. Soon after infection with HSV, intracellular levels of G actin began to rise. Figure 2 demonstrates that no increase in G actin was

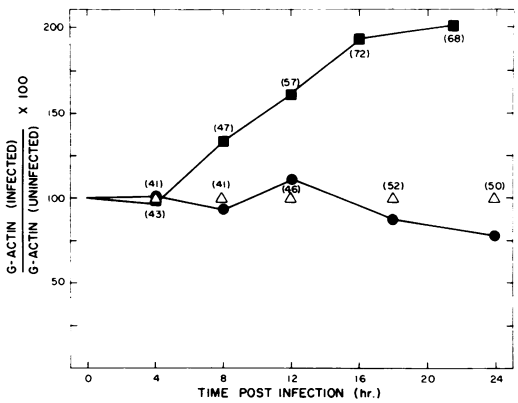

FIG. 2. G actin levels of Vero cells. At indicated times p.i., G actin levels were assessed as described in the text for uninfected cells (△) or for cells infected with HSV (■) or measles virus (●). Values shown represent the percentage of G actin levels found in infected as compared with noninfected cells. Numbers in parentheses for control and HSV-treated cultures represent G actin as a percentage of total cellular actin. These values were not determined for measles virus-infected cultures (see text).

observed during the first 4 h p.i. However, between 4 and 16 h p.i., a steady increase in G actin did occur. By 16 h p.i., intracellular G actin levels in HSV-infected cells were about twice those seen in mock-infected cultures. If Vero cells were treated with actinomycin D (20 μg/ml) immediately after the addition of postadsorption media, no such increase in G actin levels occurred. In fact, there was no disruption of the cytoskeleton at all, indicating that HSV-induced transcription is necessary for cytopathology to occur.

After infection of Vero cells with measles virus, no increase in G actin levels was observed. Rather, there was a slight decrease in the amount of G actin observed as the infection progressed. Uninfected cells generally demonstrated a slight rise in the level of G actin during the course of these experiments which might be related to cell density changes. Cultures used in these experiments were just approaching confluency at the onset of infection, and control cells were quite confluent 24 h later.

Measurement of total cell actin by sodium dodecyl sulfate slab PAGE showed no significant difference in actin amounts in either virus-infected or uninfected cells. However, amounts of certain other proteins changed in HSV- or measles virus-infected cells.

Fluorescent staining for actin filaments demonstrated that at 16 h p.i. HSV-induced microfilament disintegration was beginning to occur (Fig. 3C). This corresponded to the point in the infectious cycle when virus-specific CPE appeared. No such change in Vero cell microfilaments occurred after measles virus infection. Rather, as syncytia formation progressed, microfilament fibers extended across the giant multinucleate cells, with individual actin-containing bundles often becoming greater in length than the dimensions of the preexisting individual cells (Fig. 3B).

Effect of CB on measles virus replication. The results above show that integration of the microfilament network of individual cells into a larger but organizationally similar network was coincidental with syncytia development during measles virus infection. When measles virus-infected Vero cells were treated with 10 μg of CB per ml, syncytia formation was inhibited. Vero cells which became cuboidal in response to CB (Fig. 1D) maintained that morphology throughout the course of the measles virus infection regardless of MOI or time p.i. (≥80 h). Figure 3D shows that the prominent microfilaments were disassembled by CB. Figure 4 demonstrates that as the measles virus MOI are lowered, the yield of infectious virus in CB-treated cells decreased, whereas that in untreated cells remained relatively constant (although it did take longer for cells to succumb to measles virus infection at lower MOI). At an MOI of 0.1 or greater, there was no inhibitory effect of CB on the production of infectious measles virus; in fact, virus production was somewhat enhanced. However, as the MOI dropped, levels of infectious measles virus produced in Vero cells progressively diminished in the presence of CB. At MOI of less than 0.001, inhibition of virus production by CB exceeded 4 orders of magnitude.

To determine if the progressive inhibition of measles virus synthesis in CB-treated cells was specifically due to inhibition of cell fusion, the effect of another compound, SV-4814, was tested. This carbobenzoxy tripeptide specifically inhibits measles virus-induced cell fusion (21). The degree of inhibition of virus replication by SV-4814 was similar to that of CB at two virus concentrations (Table 1). No alteration of measles virus-infected cell microfilament structure or cellular morphology was observed in SV-4814-treated cells. Thus, it seems that agents capable of inhibiting measles virus-induced CPE are inhibitory to virus production at low MOI. Furthermore, an intact microfilament network appears to be required to produce measles virus CPE in Vero cells.

DISCUSSION

We observed that intracellular G actin levels began to increase about 4 h after the infection of Vero cells with HSV. G actin levels continued to increase throughout the course of the infection

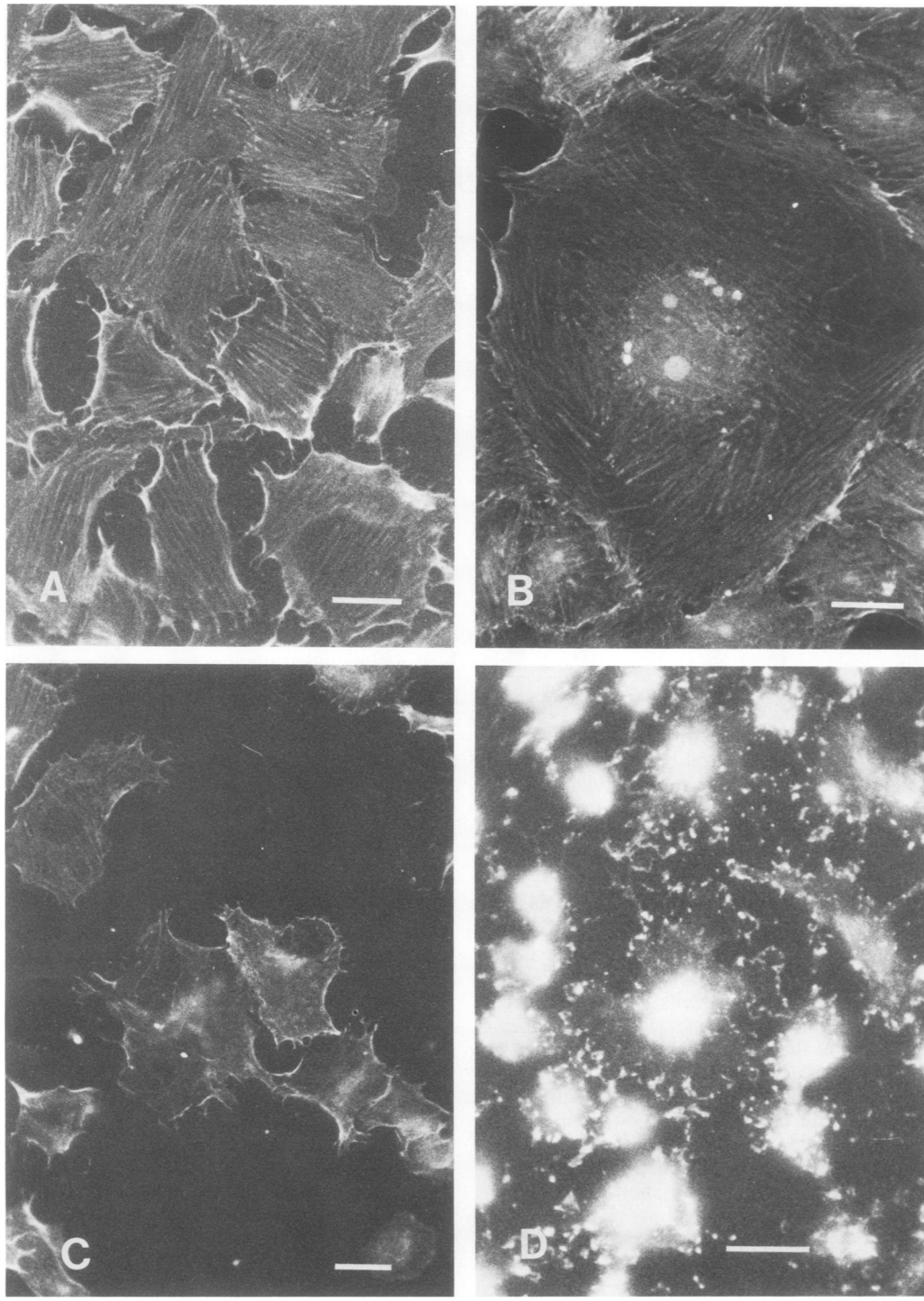

FIG. 3. Fluorescence localization of F actin in Vero cells. Cells were treated with NBD-phallacidin as described in the text. (A) Untreated cells; (B) cells infected with measles virus 22 h p.i.; (C) cells infected with HSV 16 h p.i.; (D) cells treated with 10 μg of CB per ml for 12 h. Bar, 20 μM.

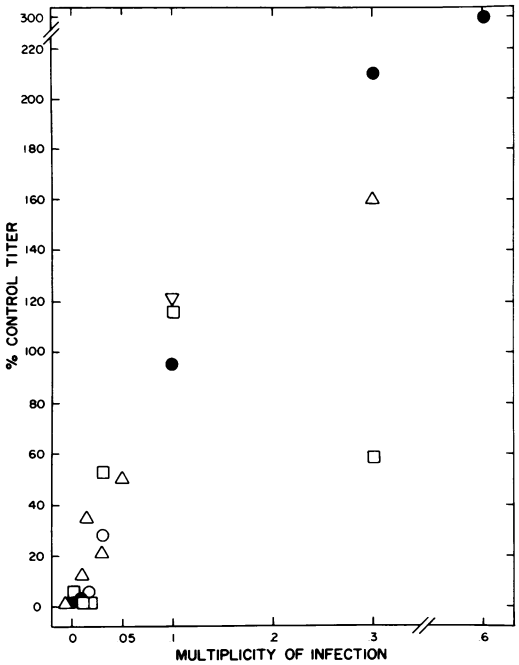

FIG. 4. Measles virus production in the presence of CB. Vero cells were either untreated or treated with 10 μg of CB per ml immediately after infection at the designated MOI. ●, △, ▽, ○, and □ represent individual experiments for which virus titers from CB-treated cells are compared with those of untreated controls.

until approximately twice the levels found in uninfected cells were measured. No such rise in the G actin levels occurred if cells were treated with actinomycin D immediately after infection, indicating that some virus-induced transcriptional event may be involved in the elevation of intracellular G actin levels. A significant rise in the G actin levels occurred well before microfilament disintegration, as assessed by either the onset of CPE by visual observation with phase-contrast optics or fluorescent staining patterns of microfilaments, using NBD-phallacidin.

A different situation occurred in Vero cells during measles virus infection, during which no rise in intracellular G actin levels was observed. Morphologically, CPE occurred. Syncitia formed and were seen by NBD-phallicidin labeling to possess prominent arrays of microfilaments which spanned the newly formed giant cells.

Total cellular actin levels of uninfected Vero cells or cells infected with either virus were not significantly different, as determined by sodium dodecyl sulfate slab PAGE. However, when total actin levels were determined, using the DNase inhibition assay, less total actin was measured after measles virus infection. It is possible that measles virus infection induces changes in Vero cells which stabilize F actin to depolymerization by GuHCl. It has been observed that a portion of the actin which undergoes polymerization as a result of chemotactic peptide stimulation in neutrophils is also resistant to GuHCl depolymerization (22).

At low MOI, a reduced amount of infectious measles virus was produced in the presence of CB, an inhibitor of microfilament assembly (16), compared with untreated cells. We feel that when all cells are not infected by functional virus particles, the mixing of cytoplasmic elements of fused cells facilitates production of greater virus yields. This is especially true with viruses prone towards the production of defective particles, such as measles virus (23). Thus, it seems predictable that cells infected with a high MOI of measles virus did not produce less virus in the presence of CB. At the highest concentrations, virus production was actually stimulated slightly, presumably because Vero cells do not die rapidly after measles virus infection when syncytia formation is inhibited (11; unpublished data). Predictably, a gradation in the inhibitory effects of CB was seen at intermediate MOI. Similarly, in other laboratories, CB has not been observed to inhibit virus replication (5, 9, 12) when a high MOI is used.

Reports concerning the fate of microfilaments after virus infections, as determined by indirect immunofluorescent antibody staining against F actin, indicate that various effects may be seen depending upon the virus being studied. Rutter and Mannweiler (24) have observed that infection of BHK-21 cells with vesicular stomatitis virus or Newcastle disease virus produced results identical to those reported here. That is, the paramyxovirus (Newcastle disease virus)

TABLE 1. Effect of syncytia-inhibiting compounds on measles virus production[a]

Agent	MOI	Titer (PFU/ml)	% Control
None	0.05	4.1×10^6	100
CB	0.05	8.1×10^5	19.7
SV-4814	0.05	8.2×10^5	20.0
None	0.005	9.5×10^6	100
CB	0.005	5.5×10^3	0.06
SV-4814	0.005	3.7×10^4	0.39

[a] Vero cells grown in 8-oz. (ca. 240-ml) prescription bottles were infected at the indicated MOI. After adsorption of virus and addition of fresh culture medium, 10 μg of CB or SV-4814 per ml was added to designated samples. Cultures were harvested by quick freezing at −70°C when untreated samples reached 100% CPE (39 h at an MOI of 0.05; 50 h at an MOI of 0.005). No CPE was ever observed in treated cells. Virus titers were assessed by the plaque assay technique described in the text.

caused no disassembly of F actin and fibers with lengths greater than those of control cell fibers were observed, whereas vesicular stomatitis virus (whose CPE results in cellular alterations similar to those induced by HSV) caused the breakdown of microfilaments after infection. Similarly, vaccinia virus causes rounding in 3T3 cells and induces a disassembly of microfilaments (19). One report disagrees with the above findings (7). These authors observed that actin-containing fibers break down during paramyxovirus infection of human lung cells but that F actin filaments are left intact after infection of these cells with either rabies virus or adenoviruses. It is not clear why the results of these authors differ from those of the others unless the cell type employed somehow affects the fluorescent patterns observed.

The role of actin or microfilaments in virus infection has never been determined. It has been proposed that microfilaments function in the movement of virus envelope proteins on the cell surface after measles virus infection (6). Recently, a close association between actin and the M protein of two other paramyxoviruses has also been described (10). Our experiments with SV-4814, an agent which inhibits measles virus CPE in Vero cells (21) without altering the cytoskeletal structure, suggest that an intact membrane network is also a prerequisite for measles virus replication at low MOI. These results suggest that membrane functions vital to paramyxovirus replication may be modulated by the actin network.

Our results demonstrate that microfilament structure is altered in response to HSV infection and imply that actin cytoskeleton function may play a role in measles virus replication, especially at low MOI. It is not likely that the inoculum of virus leading to a human diseased state approaches the levels used to study virus replication in culture. Therefore, our results suggest that a functional microfilament network would be vital to measles virus replication in patients. Because measles virus tends to produce defective particles and because its variants have been isolated from or implicated in a number of diseases of the central nervous system (20), further study of the ways host cell function contributes to virus expression should provide valuable information concerning both acute and persistent virus infection.

ACKNOWLEDGMENTS

We thank Bruce Williams for excellent technical assistance and P. R. Knight and W. W. Ackermann for their helpful discussions.

This work was supported in part by Public Health Service grant GM 28911-01 from the National Institutes of Health.

LITERATURE CITED

1. **Barak, L. S., R. R. Yocum, E. A. Nothnagel, and W. W. Webb.** 1980. Fluorescence staining of the actin cytoskeleton in living cells with 7-nitrobenz-2-oxa-1,3-diazole-phallacidin. Proc. Natl. Acad. Sci. U.S.A. **77**:980–984.
2. **Bedows, E., and F. E. Payne.** 1981. Host cell factors involved in the production of slowly sedimenting nucleocapsids in measles virus-infected cells. J. Virol. **37**:103–108.
3. **Blikstad, I., F. Markey, L. Carlsson, T. Persson, and U. Lindberg.** 1978. Selective assay of monomeric and filamentous actin in cell extracts, using inhibition of deoxyribonuclease I. Cell **15**:935–943.
4. **Clarke, M., and J. A. Spudich.** 1977. Nonmuscle contractile proteins: the role of actin and myosin in cell mobility and shape determination. Annu. Rev. Biochem. **46**:797–882.
5. **Coombs, K., E. Mann, J. Edwards, and D. T. Brown.** 1981. Effects of chloroquine and cytochalasin B on the infection of cells by Sindbis virus and vesicular stomatitis virus. J. Virol. **37**:1060–1065.
6. **Ehrnst, A., and K. G. Sundquist.** 1976. Mechanisms of appearance of viral glycoproteins at the cell surface membrane. Exp. Cell Biol. **44**:198–225.
7. **Fagraeus, A., D. L. J. Tyrrell, R. Norberg, and E. Norby.** 1978. Actin filaments in paramyxovirus-infected human fibroblasts studied by indirect immunofluorescence. Arch. Virol. **57**:291–296.
8. **Fox, J. E. B., M. E. Dockter, and D. R. Phillips.** 1981. An improved method for determining the actin filament content of nonmuscle cells by the DNase I inhibition assay. Anal. Biochem. **117**:170–177.
9. **Genty, N., and F. Busserau.** 1980. Is cytoskeleton involved in vesicular stomatitis reproduction? J. Virol. **34**:777–781.
10. **Giuffre, R. M., D. R. Tovell, C. M. Kay, and D. L. J. Tyrrell.** 1982. Evidence for an interaction between the membrane protein of a paramyxovirus and actin. J. Virol. **42**:963–968.
11. **Graves, M. C., S. M. Silver, and P. W. Choppin.** 1978. Measles virus synthesis in infected cells. Virology **86**:254–263.
12. **Griffin, J. A., and R. W. Compans.** 1979. Effect of cytochalasin B on the maturation of enveloped viruses. J. Exp. Med. **150**:379–391.
13. **Laemmli, U. K.** 1970. Cleavage of structural proteins during the assembly of the head of bacteriophage T4. Nature (London) **227**:680–685.
14. **Laub, F., M. Kaplan, and C. Gitler.** 1981. Actin polymerization accompanies Thy-1-capping on mouse thymocytes. FEBS Lett. **124**:35–38.
15. **Lowry, O. H., N. J. Rosebrough, A. L. Farr, and R. J. Randall.** 1951. Protein measurement with the Folin phenol reagent. J. Biol. Chem. **193**:265–275.
16. **MacLean-Fletcher, S., and T. O. Pollard.** 1980. Mechanism of action of cytochalasin B on actin. Cell **20**:329–341.
17. **Madansky, C. H., and M. A. Bratt.** 1978. Noncytopathic mutants of Newcastle disease virus. J. Virol. **26**:724–729.
18. **Markey, F., and L. Soriano.** 1980. Actin pools in extracts of teratocarcinoma cells, assayed by inhibition of DNase I. FEBS Lett. **110**:327–329.
19. **Meyer, R. K., M. M. Burger, R. Tschannen, and R. Schafer.** 1981. Actin filament bundles in vaccinia virus-infected fibroblasts. Arch. Virol. **67**:11–18.
20. **Morgan, E. M., and F. Rapp.** 1977. Measles virus and its associated diseases. Bacteriol. Rev. **41**:636–666.
21. **Norby, E.** 1971. The effect of a carbobenzoxy tripeptide on the biological activities of measles virus. Virology **44**:599–608.
22. **Rao, K. M. K., and J. Varani.** 1982. Actin polymerization induced by chemotactic peptide and concanavalin A in rat neutrophils. J. Immunol. **129**:1605–1607.
23. **Rima, B. K., W. B. Davidson, and S. J. Martin.** 1977. The role of defective interfering particles in persistant infection of Vero cells by measles virus. J. Gen. Virol. **35**:89–

97.
24. **Rutter, G., and K. Mannweiler.** 1977. Alterations of actin-containing structures in BHK-21 cells infected with Newcastle disease virus and vesicular stomatitis virus. J. Gen. Virol. **37**:233–242.
25. **Snabes, M. C., A. E. Boyd III, R. L. Pardue, and J. Bryan.** 1981. DNase I binding/immunoprecipitation assay for actin. J. Biol. Chem. **256**:6291–6295.
26. **Snyder, J. A., and J. R. McIntosh.** 1976. Biochemistry and physiology of microtubules. Annu. Rev. Biochem. **45**:699–720.
27. **Tyrrell, D. L. J., and H. Ehrnst.** 1979. Transmembrane communication in cells chronically infected with measles virus. J. Cell Biol. **81**:396–402.